0026-895X/06/7005-1593–1601$20.00
MOLECULAR PHARMACOLOGY
Copyright © 2006 The American Society for Pharmacology and Experimental Therapeutics
Mol Pharmacol 70:1593–1601, 2006

Vol. 70, No. 5
27714/3148940
Printed in U.S.A.

Salvicine Functions as Novel Topoisomerase II Poison by Binding to ATP Pocket

Chao-Xin Hu, Zhi-Li Zuo, Bing Xiong, Jin-Gui Ma, Mei-Yu Geng, Li-Ping Lin, Hua-Liang Jiang, Jian Ding

Division of Antitumor Pharmacology (C.-X.H., J.-G.M., M.-Y.G., L.-P.L., J.D.) and Drug Discovery and Design Center (Z.-L.Z., B.X., H.-L.J.), State Key Laboratory of Drug Research, Shanghai Institute of Materia Medica, Chinese Academy of Sciences, Shanghai, People's Republic of China

Received June 8, 2006; accepted August 15, 2006

ABSTRACT

Salvicine, a structurally modified diterpenoid quinone derived from *Salvia prionitis,* is a nonintercalative topoisomerase II (topo II) poison. The compound possesses potent in vitro and in vivo antitumor activity with a broad spectrum of anti-multidrug resistance activity and is currently in phase II clinical trials. To elucidate the distinct antitumor properties of salvicine and obtain valuable structural information of salvicine-topo II interactions, we characterized the effects of salvicine on human topo IIα (htopo IIα), including possible binding sites and molecular interactions. The enzymatic assays disclosed that salvicine mainly inhibits the catalytic activity with weak DNA cleavage action, in contrast to the classic topo II poison etoposide (VP16). Molecular modeling studies predicted that salvicine binds to the ATP pocket in the ATPase domain and superimposes on the phosphate and ribose groups. In a surface plasmon resonance binding assay, salvicine exhibited higher affinity for the ATPase domain of htopo IIα than ATP and ADP. Competitive inhibition tests demonstrated that ATP competitively and dose-dependently blocked the interactions between salvicine and ATPase domain of htopo IIα. The data illustrate that salvicine shares a common binding site with ATP and functions as an ATP competitor. To our knowledge, this is the first report to identify an ATP-binding pocket as the structural binding motif for a nonintercalative eukaryotic topo II poison. These findings collectively support the potential value of an ATP competitor of htopo IIα in tumor chemotherapy.

Human topoisomerase IIα (htopo IIα) is highly expressed in rapidly proliferating cells, and plays an essential role in replication, transcription and chromosome organization (Austin and Marsh, 1998; Wang, 2002; Carpenter and Porter, 2004). The depletion of htopo IIα eventually results in cell death (Wang, 2002; Carpenter and Porter, 2004); hence, this highly conserved nuclear enzyme is an important target for tumor chemotherapy. Approximately 50% of all the chemotherapy regimens contain at least one drug targeted to htopo IIα (Pommier et al., 1996; Hammonds et al., 1998; Wilstermann and Osheroff, 2003). All the topoisomerase II (topo II)-targeted anticancer drugs clinically used for their antitumor activities belong to topo II poisons. It is noteworthy that a wide range of topo II-targeted inhibitors are commonly classified as topo II poisons and catalytic inhibitors (Larsen et al., 2003; Wilstermann and Osheroff, 2003). Htopo IIα poisons have played an important role in chemotherapy against tumors for several decades. The most widely used topo II poisons, including etoposide, doxorubicin, and their analogs, often induce dose-limiting toxicities and multidrug resistance (MDR), resulting in treatment failure after initial effective therapy. Therefore, increasing research is focused on the development of novel htopo IIα-targeted drugs, with the aim of overcoming current limitations.

Salvicine (Fig. 1A), a structurally modified derivative of a natural diterpenequinone isolated from the traditional Chinese medicinal plant *Salvia prionitis* Hance (Labiatae), possesses potent antitumor activity both in vitro and in vivo (Qing et al., 1999; Zhang et al., 1999) and now has entered phase II clinical trials. The compound exhibits a broad spectrum of anti-MDR and antimetastatic activity (Miao et al., 2003; Lang et al., 2005). The primary molecular target of salvicine in yeast cells is eukaryotic topo II (Meng et al., 2001a). The compound was further identified as a noninter-

This work was supported by grants from the National Natural Science Foundation of China (NSFC) (30330670), the Chinese Academy of Sciences (KSCX2-SW-202), and the Ministry of Science and Technology of China (2002AA2Z346A).

Article, publication date, and citation information can be found at http://molpharm.aspetjournals.org.

doi:10.1124/mol.106.027714.

ABBREVIATIONS: htopo IIα, human topoisomerase IIα; topo II, topoisomerase II ; MDR, multidrug resistance; ICRF-187, dextrazoxan; SPR, surface plasmon resonance; DMSO, dimethyl sulfoxide; kDNA, kinetoplast DNA; TAE, Tris-acetate/EDTA; HsATPase, human topoisomerase IIα ATPase domain; ADPNP, 5′-adenylyl β,γ-imidodiphosphate; ICRF-193, 4-[(2*R*,3*S*)-3-(3,5-dioxopiperazin-1-yl)butan-2-yl]piperazine-2,6-dione.

calative poison, using extracted murine topoisomerases (Meng et al., 2001b). In human tumor cells, salvicine induces gene-specific DNA damage and triggers cell apoptosis by altering the expression of various genes, including c-*myc*, c-*fos*, c-*Jnk,* c-*jun*, and *mdr1* (Meng et al., 2001c; Miao and Ding, 2003; Lu et al., 2005). In fact, salvicine induces DNA double-strand breaks via its facilitative action on topo II–DNA binding and subsequent inhibition of pre- and post-strand topo II-mediated DNA religation without interfering in the forward cleavage steps (Meng et al., 2001b). These actions are highly correlated with its potent tumor cell growth inhibition (Meng et al., 2001c; Miao et al., 2003; Lu et al., 2005). It remains to be established whether the distinct action of salvicine on topo II is due to its structure-dominant binding mode, which is distinct from those of other topo II poisons.

Whereas eukaryotic topo II is a highly successful drug target in tumor chemotherapy, the binding sites of most nonintercalative topo II-targeted inhibitors and their precise mechanisms remain unclear. The crystal structure of ICRF-187 complexed with ATPase domain of yeast topo II reveals that the inhibitor binds to the cleft at the transient dimer interface between two ATPase promoters, and prevents successive conformational changes of the whole enzyme (Classen et al., 2003). Etoposide, a classic nonintercalative poison, binds mainly to the catalytic core domain of htopo IIα, and triggers DNA lesions in a two-drug model wherein each individual drug molecule stabilizes a strand-specific nick (Leroy et al., 2001; Bromberg et al., 2003). In general, topo II poisons are assumed to target the catalytic core domain or interact similarly with the topo II-DNA complex at the cleavage site (Robinson et al., 1993; Burden and Osheroff, 1998; Capranico et al., 2004).

In the present study, we used molecular modeling to predict the possible structural motifs of htopo IIα for salvicine binding. The modeling data were confirmed with the surface plasmon resonance (SPR)-based competitive inhibition assay. Salvicine acts as a htopo IIα poison by binding to the

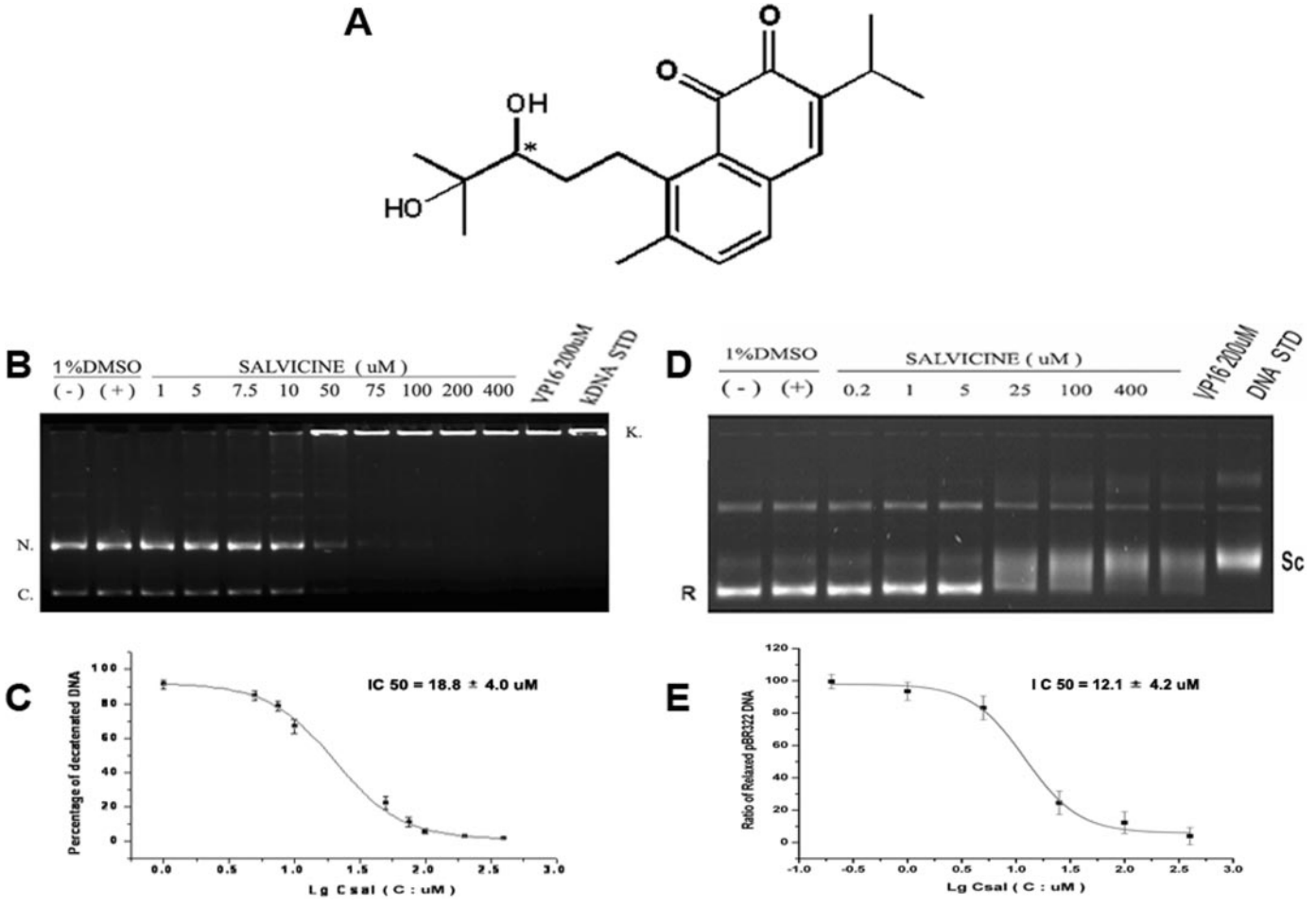

Fig. 1. Salvicine inhibits DNA decatenation and relaxation catalyzed by htopo IIα. A, chemical structure of salvicine (S, R). B, salvicine inhibits DNA decatenation catalyzed by htopo IIα. The electrophoresis assay method has been described under *Materials and Methods*. Each reaction contained the same amount of htopo IIα and the solvent of DMSO except the control reaction of kinetoplast DNA standard (kDNA STD) in the absence of htopo IIα and the control reaction of 1% DMSO (−) in the absence of DMSO. Lane SALVICINE 7.5, 10 μM, unlabeled slower running bands are intermediate size catenanes (dimers, trimers, and so forth), where intermediate levels of decatenation occurred. N., nicked, open circular decatenated kDNA; C., covalently closed circular decatenated kDNA; K. kinetoplast DNA remaining at the loading well origin. C, quantitates the effects of salvicine on DNA decatenation catalyzed by htopo IIα. Error bars represent S.D. of three independent assays. Csal, concentration of salvicine. D, salvicine inhibits DNA relaxation catalyzed by htopo IIα. Each reaction contained the same amount of htopo IIα and the solvent of DMSO except the control reaction of pBR322 supercoiled plasmid standard (DNA STD) in the absence of htopo IIα and the control reaction of 1% DMSO (−) in the absence of DMSO. E, quantitates the effects of salvicine on DNA relaxation catalyzed by htopo IIα. R and Sc. represent relaxed plasmid DNA and supercoiled plasmid DNA, respectively. The error bars represent S.D. of three independent assays.

ATP pocket in the ATPase domain. To our knowledge, this responsive binding site is the first essential structural motif identified that recognizes eukaryotic topo II poisons. Our findings should aid in elucidating the precise mechanisms involved in the antitumor activities of salvicine and enable the rational design of novel htopo II-targeted drugs.

Materials and Methods

Drugs and Chemicals. Salvicine was prepared via a two-step procedure involving epoxidation and hydration from the natural diterpenequinone isolated from the Chinese medicinal plant, *Salvia prionitis*, by the Phytochemistry Department of Shanghai Institute of *Materia Medica*, Chinese Academy of Sciences (Zhang et al., 1999). Salvicine racemoid was used in all the experiments. The purity of salvicine was greater than 99.8%, as determined by high-performance liquid chromatography. Salvicine was dissolved in DMSO at 0.1 M as a stock solution, and maintained at −20°C in the dark. [γ-^{32}P]ATP (~3000 or ~6000 Ci/mmol) was obtained from GE Healthcare (Little Chalfont, Buckinghamshire, UK). Etoposide, ATP (stored at −20°C as 20 mM stock solutions in 100% DMSO), and ethidium bromide were from Sigma (St. Louis, MO). All other chemicals were of the analytical reagent grade.

DNA Decatenation of Kinetoplast DNA. We employed the topo II assay kit from TopoGEN (Columbus, OH) to determine the effects of drugs on DNA decatenation catalyzed by htopo IIα. Htopo IIα was additionally obtained from TopoGEN. DNA decatenation assays were performed according to the manufacturer's instructions and earlier procedures (Osheroff et al., 1983; Sahai and Kaplan, 1986), with minor modifications. A standard assay was performed in a total reaction volume of 20 μl containing 50 mM Tris-HCl, pH 8.0, 120 mM KCl, 10 mM $MgCl_2$, 0.5 mM dithiothreitol, 0.5 mM ATP, 30 μg/ml bovine serum albumin, and 150 ng of kDNA. Reactions were initiated by addition of htopo IIα, and incubated for 30 min at 37°C. Sufficient enzyme was added to the assay to decatenate approximately 98 to 100% of kinetoplast DNA in the presence of the drug solvent, 1% DMSO. Various amounts of salvicine were included in separate reactions at a constant solvent volume. The reaction was terminated by the addition of 5 μl of stop solution (5% SDS, 25% Ficoll, and 0.05% bromphenol blue). Samples were resolved by electrophoresis on a 1% agarose gel containing 0.5 μg/ml ethidium bromide in TAE buffer (100 mM Tris-acetate and 2 mM EDTA, pH 8.3). DNA bands were visualized by UV and photographed on a UV transilluminator using ChemiGenius^2 (Syngene, Frederick, MD). Fluorescent bands were quantitated using Gene Tools Version 3.02 software (Syngene). The band intensity was proportional to the amount of DNA present. The 50% inhibitory concentration (IC_{50} value) for the test compound was defined as the concentration of drug in the reaction that results in a 50% decrease in the amount of decatenated DNA, including nicked circular and covalently closed circular decatenated kDNA, compared with the control reaction in which kinetoplast DNA is completely altered to decatenated DNA in the presence of 1% DMSO. All experiments to determine the IC_{50} value were performed in triplicate. The ratios of the percentage of decatenated DNA in each lane to that in the control lane (1% DMSO) were plotted against the log of the drug concentration to generate dose-response curves. Best-fit sigmoid curves were generated with Origin 6.0. IC_{50} values were calculated as the antilog of *x*-axis value of the inflection points. Error values in inflection were automatically calculated using the Origin 6.0 software.

DNA Relaxation of Supercoiled pBR322 DNA. DNA relaxation assays were performed using previous procedures (Osheroff et al., 1983; Sahai and Kaplan, 1986) with some modifications. The reactions contained 1 U of htopo IIα, 5 nM negatively supercoiled pBR322 DNA, and 1 mM ATP in a total of 20 μl of reaction buffer (50 mM Tris-HCl, pH 7.9, 135 mM KCl, 10 mM $MgCl_2$, 0.5 mM Na-EDTA, and 2.5% glycerol). A final concentration of 1% DMSO (v/v) was used in the reaction. One unit of htopo IIα was defined as the amount to relax 250 ng of corresponding substrate DNA in 30 min at 37°C. Reactions were initiated by the addition of htopo IIα, incubated for 30 min at 37°C, and terminated by the addition of 3 μl of 0.77% SDS, 77 mM Na-EDTA, pH 8.0. Samples were mixed with agarose gel loading buffer (30% sucrose, 0.5% bromphenol blue, and 0.5% xylene cyanol FF in 10 mM Tris-HCl, pH 7.9,), and subjected to electrophoresis on a 1% agarose gel in TAE buffer (100 mM Tris borate, pH 8.3, and 2 mM EDTA) containing 0.5 μg/ml ethidium bromide. DNA bands were visualized under UV, and photographed over a UV transilluminator ChemiGenius^2 (Syngene). Fluorescent bands were quantitated using Gene Tools version 3.02 software (Syngene). Band intensity was proportional to the amount of DNA present. The 50% inhibitory concentration (IC_{50}) for test compounds was defined as the amount of drug in a reaction resulting in a 50% decrease in the amount of relaxed DNA, compared with the control reaction in which supercoiled DNA is completely altered to relaxed DNA in the presence of 1% DMSO. All experiments to determine the IC_{50} values were performed in triplicate. The percentages of control relaxed DNA were plotted against the log of the concentration of the drug to generate dose-response curves, and best-fit sigmoid curves were generated with Origin 6.0. The IC_{50} value was calculated as the antilog of *x*-axis value of the inflection points. Error values within the inflection were automatically calculated using the Origin 6.0 software.

DNA Cleavage Assays. Double-stranded closed circular pRYG DNA was cleaved to form linear DNA by separating SDS-treated reaction products using ethidium bromide gel electrophoresis, according to the protocol of the topo II drug kit from TopoGEN (Columbus, OH). The 20-μl cleavage assay reaction mixture contained 4 to 8 U of htopo IIα protein, 150 ng of pRYG plasmid DNA, 0.5 mM ATP in the assay buffer [10 mM Tris-HCl, 50 mM KCl, 50 mM NaCl, 0.1 mM EDTA, 5 mM $MgCl_2$, and 2.5% (v/v) glycerol, pH 8.0], and salvicine or etoposide (2.0 μl in 10% dimethyl sulfoxide). The reaction components were added as follows: assay buffer, DNA, salvicine or etoposide, and htopo IIα. The reaction mixture was incubated at 37°C for 10 min, and quenched with 1% (v/v) SDS/25 mM Na_2EDTA. The mixture was treated with 0.25 mg/ml proteinase K (Sigma-Aldrich) at 55°C for 30 min to digest the protein. Linear pRYG DNA cleaved by htopo IIα was separated by electrophoresis (2 h for 6 V/cm) on a TAE ethidium bromide (0.5 μg/ml) agarose gel [1% (w/v)].

Molecular Docking. The crystal structure of the ATPase domain of htopo IIα in complex with ADPNP was retrieved from the Brookhaven Protein Data Bank (PDB entry 1ZXM) (Wei et al., 2005). The hydrogen atoms of the protein were added using the software package Sybyl 6.8 (Tripos Associates Inc., St. Louis, MO). Protein atom types and potentials were assigned according to the Amber 4.0 force field with Kollman-united-atom charges (Weiner et al., 1984) encoded in Sybyl 6.8. The initial structures of salvicine, ATP, and ADPNP were optimized using the Tripos force field with Gasteiger-Hücker charges. The Powell method was used for energy minimization using an 8-Å nonbonded cutoff and an energy convergence gradient value of 0.001 kcal/(mol · Å).

The advance docking program AutoDock 3.0.3 (http://www.scripps.edu/mb/olson/doc/autodock/) was used to dock ligands to the htopo IIα ATPase domain. The Lamarckian genetic algorithm (Morris et al., 1998) was applied to analyze protein-ligand interactions. A Solis and Wets local search (Morris et al., 1998) was performed for energy minimization on a user-specified proportion of the population. The docked structures of the ligands were generated after a reasonable number of evaluations. The whole docking operation could be stated as follows:

1. Each ligand molecule was checked for polar hydrogens and assigned for partial atomic charges, and the atomic solvation parameters were also assigned for the protein. The kinds of atomic charges were taken as Kollman-united-atom for protein and Gasteiger-Hücker charges for the ligands.

2. The three-dimensional grid with 60 × 60 × 60 points and a spacing of 0.375 Å was created by the AutoGrid algorithm to evaluate the binding energies between the ligands and the proteins. In this stage, the protein was embedded in the three-dimensional grid, and a probe atom was placed at each grid point. The affinity and electrostatic potential grid were calculated for each type of atom in the ligands. The energetics of a particular ligand configuration was found by trilinear interpolation of affinity values and electrostatic interaction of the eight grid points surrounding each of the atoms in a ligand.
3. A series of the docking parameters were set on. Not only the atom types but also the generations and the number of runs for the Lamarckian genetic algorithm were edited and properly assigned according to the requirement of the Amber force field. The number of generations, energy evaluations, and docking runs were set to 37×10^3, 1.5×10^6, and 20, respectively.

All modeling and calculations were performed on a Silicon Graphics Origin3200 workstation with four CPUs.

Identification and Purification of the Human Topoisomerase IIα ATPase Domain. The HsATPD plasmid and yeast strain, BCY123, for expressing human topoisomerase IIα ATPase domain (HsATPase) were presented by Professor Tao-shih Hsieh (Department of Biochemistry, Duke University Medical Center, Durham, NY). HsATPase was overexpressed and purified as described previously (Hu et al., 2002), with some modifications. To purify HsATPase, the cleared lysate prepared from a 10-liter culture was passed through a 6-ml Ni^{2+}-nitrilotriacetic acid column (QIAGEN, Valencia, CA) in the presence of 20 mM imidazole, pH 8.0, and 250 mM NaCl was included in all buffers throughout the purification. After washing with 80 ml of 30 mM imidazole solution, stepwise concentrations of 40, 60, 80, 120, 160, 200 and 250 mM imidazole were used to elute the protein in a volume of 18 ml at each step. The His-tagged topo II protein was eluted between 80 and 120 mM imidazole. Peak fractions containing target protein were combined and diluted with sampling solution (50 mM Tris-HCL, pH7.8, 10% glycol, 0.2 M NaCl). The solutions were further purified using HQ and HE column chromatography (GE Healthcare). Final peak fractions were divided into two parts and dialyzed against either HEPES buffer (20 mM HEPES, 150 mM NaCl, 5 mM EDTA, and 0.005% surfactant P20, pH 7.4) or storage buffer [10 mM Tris acetate, pH 7.8, 50 mM KAc, 5 mM $Mg(Ac)_2$, and 50% glycerol]. Before the ATP-hydrolysis assay, proteins were concentrated and exchanged with buffer comprising 10 mM Tris-acetate, pH 7.9, using a Microcon centrifugal device (Millipore Corp., Bedford, MA). The purity of expressed protein was further determined by SDS-polyacrylamide gel electrophoresis and high-performance liquid chromatography. The ATP hydrolysis activity of the purified protein was determined, as described previously (Osheroff et al., 1983; Hu et al., 2002) (see below).

Surface Plasmon Resonance Analysis. The SPR assay was performed at 25°C using a Biacore 3000 instrument (Biacore AB, Uppsala, Sweden). Proteins were immobilized onto CM5 sensor chips after activation of the surface carboxyl groups by the addition of a mixture of *N*-hydroxysuccinimide (0.05 M in H_2O) and 1-ethyl-3-(3-diaminopropyl)carbodiimide (0.2 M in H_2O) (35 μl; Biacore amine coupling kit), according to the manufacturer's instructions. HsATPase (40 ug/ml) diluted in 10 mM sodium acetate, pH 5.5, was injected in 20- to 50-μl aliquots across the surface of the chip until a response of 6000 to 7000 resonance units was reached. Esters were deactivated by an injection of 35 μl of ethanolamine, followed by 50 μl of regeneration buffer (2 M KCl). The system was reprimed with running buffer (20 mM HEPES, 150 mM NaCl, 5 mM EDTA, and 0.005% P20, pH 7.4). The flow rate was increased to 20 μl/min, and a range of concentrations of salvicine, ATP, and ADP were allowed to flow across the surface. The dilution buffer for ligands is similar to running buffer with the addition of 0.1% DMSO and 10 mM $MgCl_2$. Sensorgrams were processed using the automatic correction for nonspecific bulk refractive index effects. Equilibrium constants (K_D) for evaluating protein-ligand binding affinity were determined using the steady-state affinity fitting analysis.

ATP Hydrolysis in the Absence of DNA. ATPase assays were performed as described previously (Osheroff et al., 1983; Hu et al., 2002), with some modifications. ATP hydrolysis reactions contained 50 to 300 nM HsATPase, 1 mM [γ-^{32}P]ATP (3000 Ci/mmol stock), and 0 or 25, 50, or 100 μM salvicine (1% final DMSO) in a total volume of 20 μl of reaction buffer. The reaction mixture contained 10 mM Tris acetate, pH 7.9, 120 mM KCl, 10 mM $MgCl_2$, and 0.5 mM dithiothreitol. The concentrations of ATP used were 0.25, 0.5, 0.75, 1.0, 1.5, and 2.0 mM, respectively. Reactions were initiated by the addition of HsATPase, and incubated at 37°C. Samples (2.5 μl) were removed at intervals up to 20 min, and spotted on polyethylenimine-impregnated thin-layer cellulose chromatography plates (J. T. Baker Inc., Phillipsburg, NJ). Plates were developed by chromatography in freshly prepared 400 mM NH_4HCO_3 and analyzed by autoradiography. Radioactive areas corresponding to free inorganic phosphate released by ATP hydrolysis were dissected and quantitated by scintillation counting. In all experiments, only data from the linear range of ATP hydrolysis were used to calculate the reaction rates. Data were processed and fitted with the software Origin 6.0. (OriginLab Corp., Northampton, MA)

Results

Effects of Salvicine on Human Topoisomerase IIα Activity. Salvicine has been identified as a nonintercalative topo II poison, using extracted murine topoisomerases and a yeast cell model (Meng et al., 2001a,b). However, the mode of action of salvicine on htopo IIα, which represents the major topo II isoform present in rapidly proliferating human cells, remains to be established. As indicated in Fig. 1, B and D, salvicine inhibited the htopo IIα-catalyzed relaxation of pBR322 DNA and decatenation of kDNA. Gel quantitative assays disclosed IC_{50} values of 12.1 ± 4.2 and 18.8 ± 4.0 μM for salvicine-mediated inhibition of DNA relaxation and decatenation, respectively, (Fig. 1, C and E).

Results from the DNA cleavage assay performed using htopo IIα showed that 400 μM salvicine induced weak DNA cleavage that was approximately 10% of that generated by 200 μM etoposide (data not shown).

Salvicine Bound to the ATP Pocket of Human Topoisomerase IIα. To identify the binding site of salvicine to the ATPase domain, docking simulation was performed using AutoDock 3.0.3. To obtain the appropriate docking parameters, ATP and ADPNP were initially docked with the ATPase domain of htopo IIα. The result indicated that ATP and ADPNP lay in the ATP binding site (Fig. 2), suggesting that the parameters for docking are reliable. Further studies demonstrated that salvicine might bind at the ATP site of htopo IIα ATPase domain (Fig. 2). As indicated in the interaction model between salvicine and htopo IIα ATPase domain, salvicine formed strong hydrogen bonds with the enzyme (Fig. 2B): two carbonyl groups in naphthoquinone of salvicine hydrogen bound to residue Asn150; the 4-hydroxyl group in long side chain salvicine formed several hydrogen bonds with Arg162, Asn163, and Gly164; and the 5-hydroxyl group at the terminal also formed hydrogen bonds with Glu87, Gly166, and Gln376. In addition, salvicine was stabilized in the ATP site by hydrophobic interactions. Remarkably, the long side chain of salvicine overlapped with the phosphate and ribose moieties of ANPNP in the ATP binding site (Fig. 2A). All these indicated that salvicine might compete with ATP for binding to the ATP binding site of htopo IIα.

Salvicine Bound to the ATPase Domain in Human Topoisomerase IIα; Identification and Purification of the Human Topoisomerase IIα ATPase Domain. It is predicted that salvicine binds at the ATP binding pocket of the htopo IIα ATPase domain. To determine whether salvicine binds to the ATPase domain of htopo IIα, htopo IIα ATPase domain was initially prepared and purified. The 46-kDa fragment of the ATPase domain of htopo IIα, HsATPase, was overexpressed in a protease-deficient yeast strain, BCY123, purified to more than 96% homogeneity (Fig. 3A), and HsATPase activity was monitored. The HsATPase obtained significantly hydrolyzed ATP in a dose-dependent manner (Figs. 3B and 4A), indicative of active enzyme.

Salvicine Bound to the Human Topoisomerase IIα ATPase Domain. Next, we applied the SPR assay to analyze whether salvicine bound HsATPase. With HsATPase immobilized onto the hydrophilic carboxymethylated dextran matrix of the sensor chip CM5, a series of buffers containing different concentrations of salvicine or ATP and ADP, natural ligands of htopo IIα, were injected over the chip surface. Real-time binding sensograms were recorded. General fitting and steady-state binding affinities were calculated using BIAeval 3.1 software. Interactions of salvicine, ATP, and ADP with HsATPase were dose-dependent (Fig. 3C). Steady-state affinity analyses disclosed a K_D value of 7.43×10^{-5} M for salvicine binding, which is approximately 2 or 3 orders of magnitude higher than the K_D value $7.83 \pm 0.58 \times 10^{-3}$M of ATP or $1.50 \pm 0.10 \times 10^{-2}$ M of ADP.

Salvicine Inhibited HsATPase-Catalyzed ATP Hydrolysis in the Absence of DNA via Competition with ATP. To test the docking prediction, we investigated whether salvicine could inhibit HsATPase-catalyzed ATP hydrolysis. Here, the Lineweaver-Burk plot was preferentially used. As indicated in Fig. 4A, the effects of various concentrations of

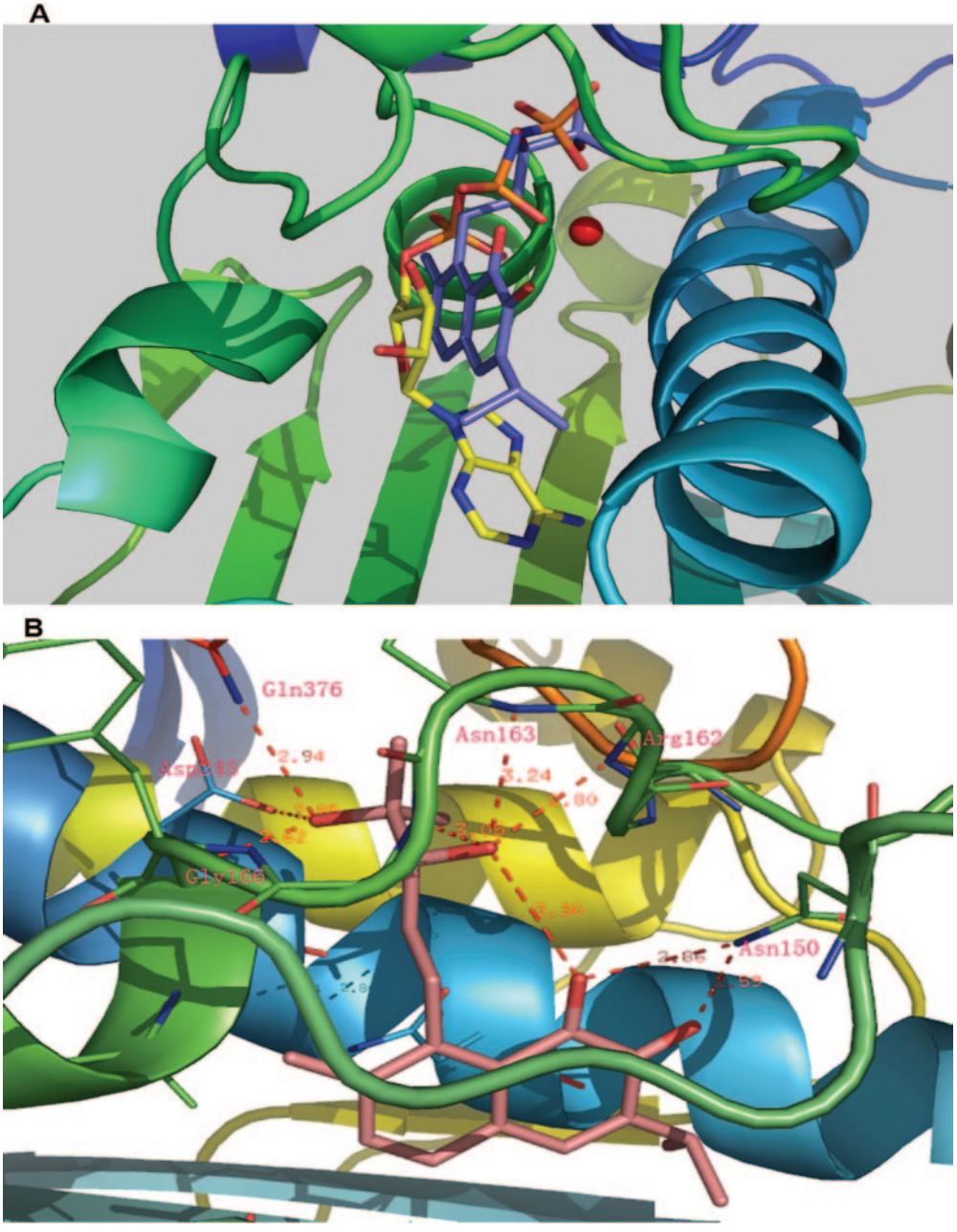

Fig. 2. The docking prediction of salvicine bound to the ATP binding site of htopo IIα. A, the ADPNP (in yellow, blue, and deep salmon) and salvicine (in blue and salmon) were superimposed in the binding site, and salvicine overlapped with ANPNP at the phosphate and ribose moieties. The red ball represents Mg^{2+}. B, the detailed binding interactions between salvicine (in salmon). The dashed lines represent the hydrogen bonds between salvicine and residues in ATP binding site of htopo IIα. The pictures were prepared using the PyMol programs (http://pymol.sourceforge.net/).

ATP on salvicine-mediated inhibition of HsATPase-catalyzed ATP-hydrolysis activity in the absence of DNA were investigated. The double reciprocal Lineweaver-Burk plot revealed that salvicine was an ATP-competitive inhibitor of HsATPase.

Salvicine Blocked DNA Decatenation in an ATP-Dependent Manner. To further confirm whether the ATP pocket was the only binding cavity within the htopo IIα enzyme for salvicine, we performed a competition inhibition assay on DNA decatenation catalyzed by htopo IIα at different concentrations of ATP. The IC_{50} values of salvicine inhibition of DNA decatenation by htopo IIα were determined at different ATP concentrations, as described under *Materials and Methods*. The IC_{50} value for salvicine-mediated inhibition of DNA decatenation was affected by the ATP concentration during catalysis by htopo IIα. With the rise in ATP concentration from 0.5 to 1.5 mM, the IC_{50} values for salvicine increased from 22 μM to 101 μM (Fig. 4, B and C). The curve patterns (Fig. 4C) are similar to that of a competitive antagonist, which binds to the same receptor pocket as the agonist (Zhou, 1999).

Discussion

Salvicine, a nonintercalative topo II poison identified from enzymatic studies of extracted murine topoisomerases, inhibits the decatenation and relaxation of htopo IIα. It is noteworthy that although salvicine is a weak poison of htopo IIα in vitro relative to such known poisons as etoposide and doxorubicin, the compound triggers potent double-strand breaks and apoptosis in vivo (Meng et al., 2001b,c; Miao and Ding, 2003; Lu et al., 2005). This action of salvicine on htopo IIα may be due to a distinct, structure-dominant molecular mechanism. Elucidation of salvicine-htopo IIα interactions offers a clear view of the structural relationship between salvicine and htopo IIα and the antitumor mechanisms of salvicine, which should facilitate the design of new htopo II-targeted drug types.

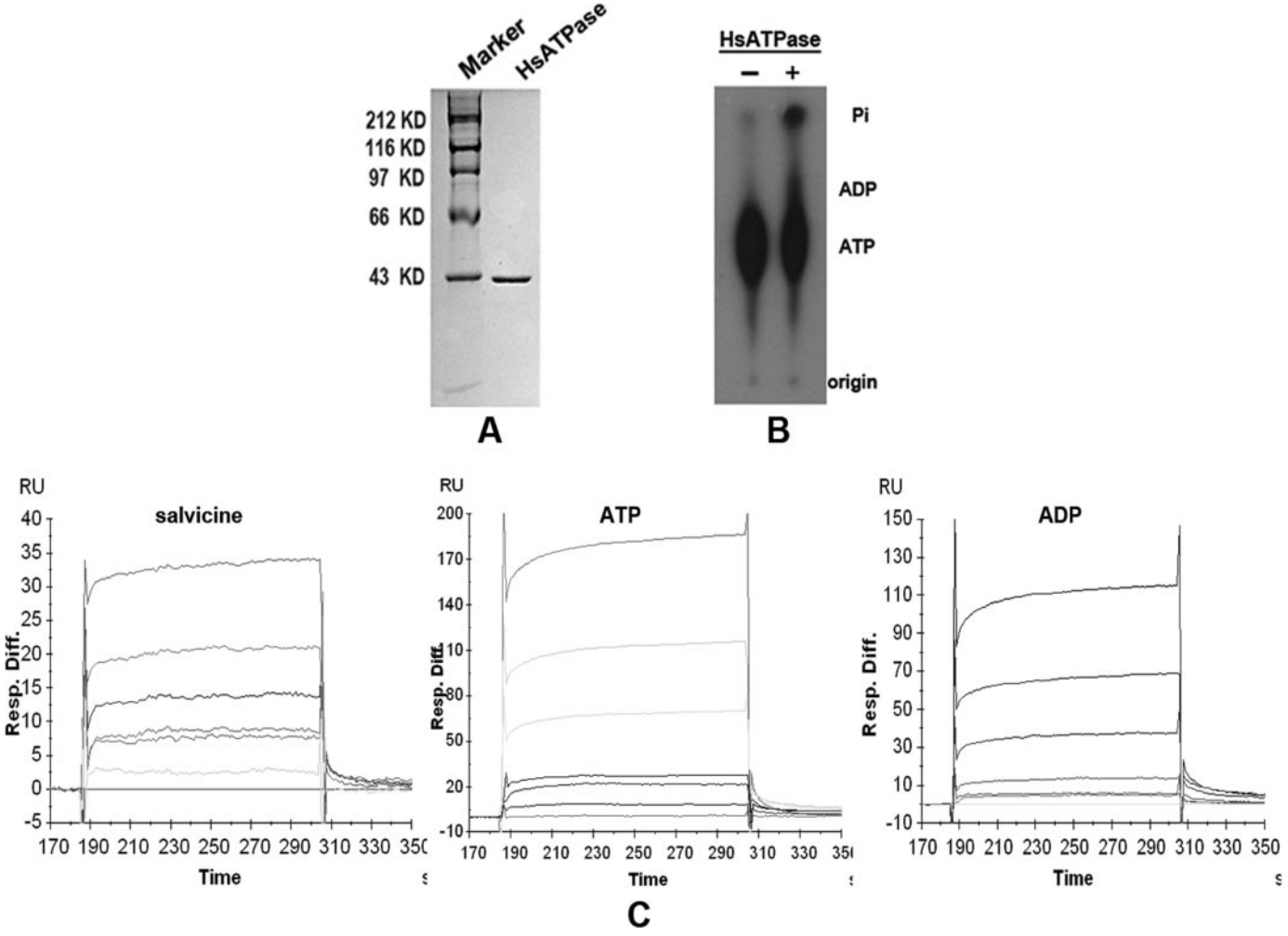

Fig. 3. Salvicine binds to HsATPase dose dependently. A and B, identification of HsATPase. A, 2 μg each of molecular size markers and purified HsATPase were run in a 10% SDS-polyacrylamide gel electrophoresis and stained with Coomassie brilliant blue. B, the activity of purified HsATPase were assayed in a reaction of 20-μl total volume containing 100 nM HsATPase, 2.0 μCi [γ-^{32}P]ATP, and 1 mM ATP. Reaction solution (2.5 μl) was removed and spotted at 10 min incubated at 37°C onto the *origin* of polyethyleneimine-impregnated thin layer cellulose chromatography plates. Pi (phosphate) and ADP are the hydrolysate of *ATP*. C, representive sensorgrams of salvicine, ATP and ADP binding to and dissociating from HsATPase. The binding experiments were performed on a Biacore 3000 with a flow rate of 20 μl/min at 25°C and a running buffer of 20 mM HEPES, 150 mM NaCl, 5 mM EDTA, and 0.005% P20. The concentration series from top to bottom: salvicine, 100, 50, 25, 12.5, 6.25, 3.125, and 0 μM; ATP, 5, 2.5, 1.25, 0.625, 0.3125, 0.15625, and 0 mM; ADP, 5, 2.5, 1.25, 0.625, 0.3125, 0.15625, and 0 mM.

The clarification of the binding pocket and precise mechanism of interactions between eukaryotic topoisomerase II and poisons or catalytic inhibitors is generally difficult due to the limited techniques, huge size of the triple/quadruple complex of ligand-topo II-ATP-DNA, and the requirement of large amount of enzyme. In particular, substantial conformational changes in the topo II and ATP-topo II-DNA complex affect formation of the binding pocket of a poison or a catalytic inhibitor during catalysis (Berger et al., 1996; Classen et al., 2003; Wei et al., 2005).

Several studies have suggested that the cleavage site, α_4 helix of the CAP-like domain of topo II and the broken duplex may constitute the binding cavity of classic nonintercalative poisons despite the lack of direct crystal structural evidence (Burden and Osheroff, 1998; Capranico et al., 2004). ICRF-187, a typical bisdioxopiperazines compound, was disclosed to bind to the cleft between the dimer of the ATPase domain of yeast topo II (Classen et al., 2003). Likewise, structures of gyrase B fragments complexed with ADPNP, novobiocin, chlorobiocin, and cyclothialidine reveal competitive inhibition with ATP (Boehm et al., 2000). With the rapid progress in molecular simulation alongside the characterized crystal structures, it has become easier to predict the possible binding information between ligands and receptors via molecular docking. Among the molecular docking studies performed to date, structure-based drug design targeting the ATP pocket of DNA gyrase B, the prokaryotic counterpart of the eukaryotic topoisomerase II ATPase domain, has proved successful in discovering a 10-fold more potent inhibitor than novobiocin (Boehm et al., 2000). Using the crystal structure of the htopo IIα ATPase domain, we found that salvicine provides a polar hydroxyl group for binding to the ATPase domain, similar to the phosphate group of ADPNP or ATP. Moreover, the naphthoquinone ring of salvicine adopts a position close to the ribose moiety in the ATP structure. These findings stand in contrast to data on novobiocin and cyclothialidine, in which the overlapping regions of binding sites were the novioose sugar of novobiocin for the adenine ring of ADPNP and

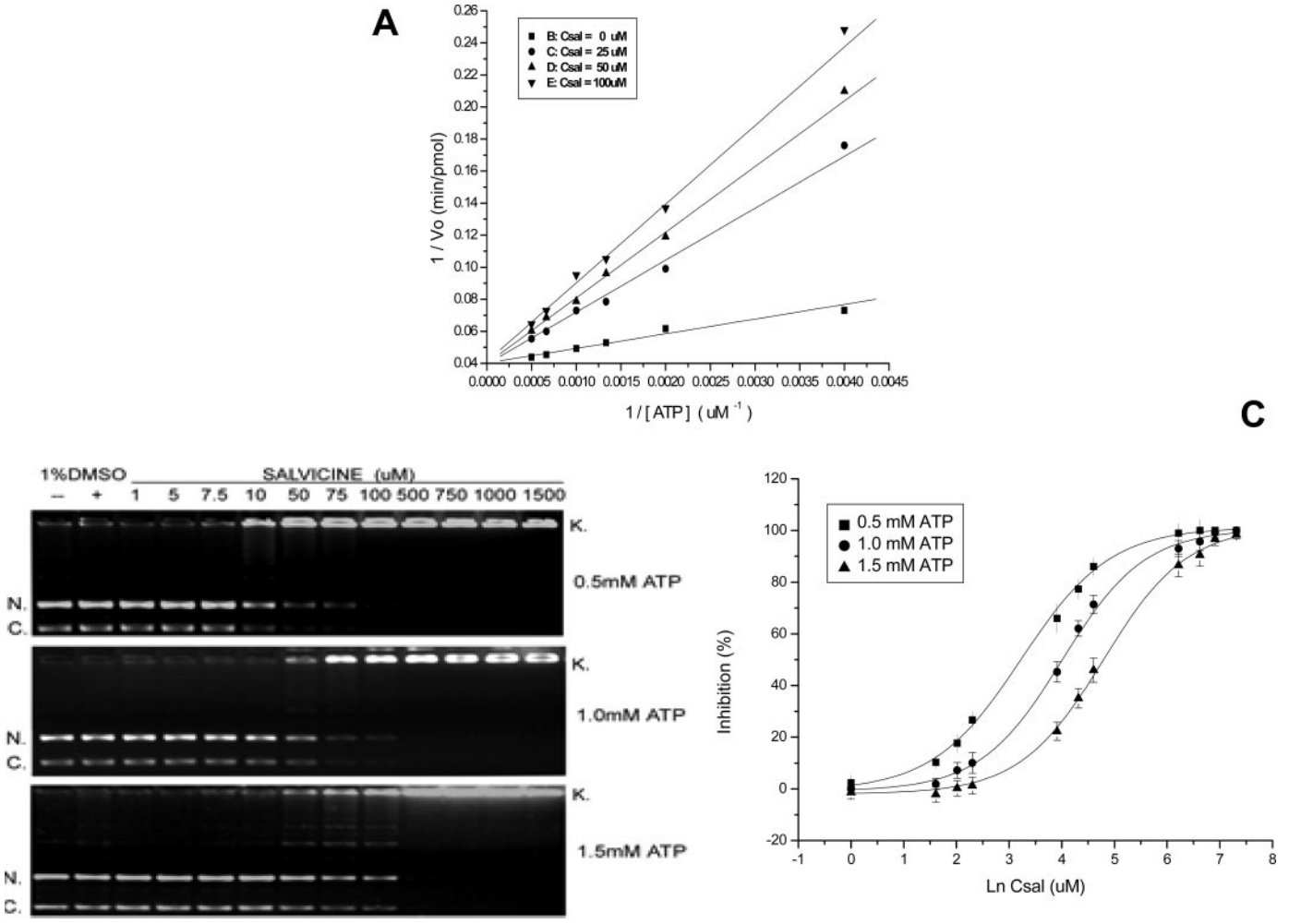

Fig. 4. Salvicine inhibits HsATPase and whole enzyme htopo IIα by competing with ATP. A, a double-reciprocal plot for ATP-hydrolysis activity of HsATPase in the absence of DNA. Various concentrations of ATP in the absence (■) or presence of salvicine (●, 25 μM; ▲, 50 μM; ▼, 100 μM) were incubated at 37°C with 300 nM HsATPase in reaction buffer. B and C, the IC_{50} of salvicine inhibiting DNA decatenation catalyzed by htopo IIα depends on the concentration of ATP. B shows the effects of salvicine on DNA decatenation catalyzed by htopo IIα at 0.5, 1.0, and 1.5 mM ATP, respectively. The electrophoresis assay method has been described under *Materials and Methods*. Each reaction contained the same amount of htopo IIα and the solvent of DMSO except the control reaction of 1% DMSO (−) in the absence of DMSO. N., nicked, open circular decatenated kDNA; C., covalently closed circular decatenated kDNA; K. kinetoplast DNA remaining at the loading well origin. *C* quantitates the effects of salvicine on DNA decatenation catalyzed by htopo IIα at different concentration of ATP. The fit data gave IC_{50} values of 22 ± 4, 45 ± 7, and 101 ± 15 μM for reaction containing 0.5 (■), 1.0 (●), and 1.5 (▲) mM ATP, respectively. Error bars represent S.D. of three independent assays. Csal, concentration of salvicine. The error bars represent the deviation from the mean for data from three separate experiments.

the resorcinol ring of cyclothialidine for the adenine ring of ADPNP, respectively (Boehm et al., 2000). Thus, these findings indicate that the action of salvicine on topo II is distinct from that of conventional ATP competitors. Moreover, in further support of this theory, salvicine failed to dock into the cavity formed by the cleavage site and α4 helix of the CAP-like domain of htopo IIα, commonly assumed as the binding site of nonintercalative topo II poisons (Burden and Osheroff, 1998; Capranico et al., 2004; Christmann-Franck, 2004).

The SPR biosensor assay is an accurate method to identify the interactions between ligands and receptors. In the current study, data from the SPR assay showed that salvicine exhibits significantly higher affinity for the ATPase domain of htopo IIα than ATP and ADP. It is noteworthy that the finding that ATP competitively inhibits salvicine-ATPase interactions implies that salvicine shares a common binding site(s) with ATP, at least in part.

The key steps in the topo II catalysis reaction include hydrolysis of ATP coupled with DNA strand passage and subsequent DNA breakage-reunion reactions (Roca and Wang, 1992; Wang, 2002; Larsen et al., 2003; Wilstermann and Osheroff, 2003). It is possible that drugs that interact with the ATP-binding or related sites of topo II have a profound effect on enzyme activity (Classen et al., 2003; Larsen et al., 2003; Maxwell and Lawson, 2003; Wilstermann and Osheroff, 2003). This theory was highlighted by the finding that bisdioxopiperazines, including ICRF-187, ICRF-193, and their analogs, bind to the closed-clamp form of the enzyme and prevent its conversion to the open-clamp form, in which the formation and transition of clamp conformation is dependent on ATP and ATP hydrolysis (Roca et al., 1994; Huang et al., 2001; Classen et al., 2003). Moreover, the nonhydrolyzable ATP analog ADPNP traps DNA-topo II in a closed-clamp conformation, although ADPNP binds to the ATP binding pocket by competing with ATP (Roca and Wang, 1992; Morris et al., 1999; Wang et al., 2001). In view of these findings, we propose that salvicine poisons htopo IIα by trapping the closed-clamp conformation of the htopo IIα-DNA complex. Of course, further investigation is required to confirm this theory.

Here, we showed for the first time that salvicine binding overlapped with that of ATP. Moreover, salvicine functioned as an ATP competitor and exhibited activity distinct from that of other classic topo II poisons. Given that ATP competitors of gyrase B have been pharmaceutically successful (Boehm et al., 2000), our finding raises the hope of the agents targeting ATP pocket of htopo IIα in tumor chemotherapy and has implications for future drug design, the molecular mechanism of both eukaryotic topo II and its ATP competitor.

Acknowledgments

We are grateful to Dr. and Professor Tao-shih Hsieh (Department of Biochemistry, Duke University Medical Center) for the gift of plasmid HsATPD and yeast strain BCY123. We thank Professor Jinsheng Zhang for providing salvicine. We also thank Dr. Haibin Luo and Professor Xu Sheng for assistance in binding assay with BIAcore 3000.

References

Austin CA and Marsh KL (1998) Eukaryotic DNA topoisomerase IIβ. *BioEssays* **20:**215–226.

Berger JM, Gamblin SJ, Harrison SC, and Wang JC (1996) Structure and mechanism of DNA topoisomerase II. *Nature (Lond)* **379:**225–232.

Boehm HJ, Boehringer M, Bur D, Gmuender H, Huber W, Klaus W, Kostrewa D, Kuehne H, Luebbers T, Meunier-Keller N, et al. (2000) Novel inhibitors of DNA gyrase: 3D structure based biased needle screening, hit validation by biophysical methods, and 3D guided optimization. A promising alternative to random screening. *J Med Chem* **43:**2664–2674.

Bromberg K_D, Burgin AB, and Osheroff N (2003) A two-drug model for etoposide action against human topoisomerase IIα. *J Biol Chem* **278:**7406–7412.

Burden DA and Osheroff N (1998) Mechanism of action of eukaryotic topoisomerase II and drugs targeted to the enzyme. *Biochim Biophys Acta* **1400:**139–154.

Capranico G, Zagotto G, and Palumbo M (2004) Development of DNA topoisomerase-related therapeutics: a short perspective of new challenges. *Curr Top Med Chem* **4:**335–345.

Christmann-Franck S, Bertrand HO, Goupil-Lamy A, Garabedian PA, Mauffret O, Hoffmann R, and Fermandjian S (2004) Structure-based virtual screening: an application to human topoisomerase IIα. *J Med Chem* **47:**6840–6853.

Carpenter AJ and Porter AC (2004) Construction, characterization, and complementation of a conditional-lethal DNA topoisomerase IIalpha mutant human cell line. *Mol Biol Cell* **15:**5700–5711.

Classen S, Olland S, and Berger JM (2003) Structure of the topoisomerase II ATPase region and its mechanism of inhibition by the chemotherapeutic agent ICRF-187. *Proc Natl Acad Sci USA* **100:**10629–10634.

Hammonds TR, Maxwell A, and Jenkins JR (1998) Use of a rapid throughput in vivo screen to investigate inhibitors of eukaryotic topoisomerase II enzymes. *Antimicrob Agents Chemother* **42:**889–894.

Huang C, Gao H, Yamasaki EF, Grabowski DR, Liu S, Shen LL, Chan KK, Ganapathi RR, and Snapka RM (2001) Topoisomerase II poisoning by ICRF-193. *J Biol Chem* **276:**44488–44494.

Hu T, Sage H, and Hsieh T (2002) ATPase Domain of Eukaryotic DNA Topoisomerase II: inhibition of ATPase activity by the anti-cancer drug bisdioxopiperazine and ATP/ADP-induced dimerization. *J Biol Chem* **277:**5944–5951.

Lang JY, Chen H, Zhou J, Zhang YX, Zhang XW, Li MH, Lin LP, Zhang JS, Waalkes MP, and Ding J (2005) Antimetastatic effect of salvicine on human breast cancer MDA-MB-435 orthotopic xenograft is closely related to Rho-dependent pathway. *Clin Cancer Res* **11:**3455–3464.

Larsen AK, Escargueil AE, and Skladanowski A (2003) Catalytic topoisomerase II inhibitors in cancer therapy. *Pharmacol Ther* **99:**167–181.

Leroy D, Kajava AV, Frei C, and Gasser SM (2001) Analysis of etoposide binding to subdomains of human DNA topoisomerase IIα in the absence of DNA. *Biochemistry* **40:**1624–1634.

Lu HR, Meng LH, Huang M, Zhu H, Miao ZH, and Ding J (2005) DNA damage, c-myc suppression and apoptosis induced by the novel topoisomerase II inhibitor, salvicine, in human breast cancer MCF-7 cells. *Cancer Chemother Pharmacol* **55:**286–294.

Maxwell A and Lawson DW (2003) The ATP-binding site of type II topoisomerases as a target for antibacterial drugs. *Curr Top Med Chem* **3:**283–303.

Meng LH, He XT, Zhang JS, and Ding J (2001a) DNA Topoisomerase II as the primary cellular target for salvicine in *Saccharomyces cerevisiae*. *Acta Pharmacol Sin* **22:**741–746.

Meng LH, Zhang JS, and Ding J (2001b) Salvicine, a Novel DNA topoisomerase II inhibitor, exerting its effects by trapping enzyme-DNA cleavage complexes. *Biochem Pharmacol* **62:**733–741.

Meng LH, Zhang JS, and Ding J (2001c) Induction of bulk and c-myc P2 promoter-specific DNA damage by an anti-topoisomerase II agent salvicine is an early event leading to apoptosis in HL-60 cells. *FEBS Lett* **501:**59–64.

Miao ZH, Tang T, Zhang YX, Zhang JS, and Ding J (2003) Cytotoxicity, apoptosis induction and downregulation of MDR-1 expression by the anti-topoisomerase II agent, salvicine, in multidrug-resistant tumor cells. *Int J Cancer* **106:**108–115.

Miao ZH and Ding J (2003) Transcription factor C-Jun activation represses Mdr-1 gene expression. *Cancer Res* **63:**4527–4532.

Morris GM, Goodsell DS, Halliday RS, Huey R, Hart WE, Belew RK, and Olson AJ (1998) Automated docking using a Lamarckian genetic algorithm and an empirical binding free energy function. *J Comput Chem* **19:**1639–1662.

Morris SK, Harkins TT, Tennyson RB, and Lindsley JE (1999) Kinetic and thermodynamic analysis of mutant type II DNA topoisomerases that cannot covalently cleave DNA. *J Biol Chem* **274:**3446–3452.

Osheroff N, Shelton ER, and Brutlag DL (1983) DNA topoisomerase II from *Drosophila melanogaster*: kinetics of relaxation of supercoiled DNA. *J Biol Chem* **258:**9536–9543.

Pommier Y, Fesen MR, and Goldwasser F (1996) in *Cancer Chemotherapy and Biotherapy: Principles and Practice* (Chabner BA and Longo DL eds) pp 435–461, Lippincott-Raven Publishers, Philadelphia.

Qing C, Zhang JS, and Ding J (1999) In vitro cytotoxicity of salvicine, a novel diterpenoid quinone. *Zhongguo Yao Li Xue Bao* **20:**297–302.

Robinson MJ, Corbett AH, and Osheroff N (1993) Effects of topoisomerase II-targeted drugs on enzyme-mediated DNA cleavage and ATP hydrolysis: evidence for distinct drug interaction domains on topoisomerase II. *Biochemistry* **32:**3638–3643.

Roca J, Ishida R, and Berger JM, Andoh T, and Wang JC (1994) Antitumor bisdioxopiperazines inhibit yeast DNA topoisomerase II by trapping the enzyme in the form of a closed protein clamp. *Proc Natl Acad Sci USA* **91:**1781–1785.

Roca J and Wang JC (1992) The capture of a DNA double helix by an ATP-dependent protein clamp: a key step in DNA transport by type II DNA topoisomerases. *Cell* **71:**833–840.

Sahai BM and Kaplan JG (1986) A quantitative decatenation assay for type II topoisomerases. *Anal Biochem* **156:**364–379.

Wang H, Mao Y, Zhou N, Hu T, Hsieh TS, and Liu LF (2001) ATP-bound topoisomerase II as a target for antitumor drugs. *J Biol Chem* **276:**15990–15995.

Wang JC (2002) Cellular roles of DNA topoisomerases: a molecular perspective. *Nat Rev Mol Cell Biol* **3:**430–440.

Wei H, Ruthenburg AJ, Bechis SK, and Verdine GL (2005) Nucleotide-dependent domain movement in the ATPase domain of a human type IIa DNA topoisomerase. *J Biol Chem* **280:**37041–37047.
Weiner SJ, Kollman PA, Case DA, Singh C, Ghio G, Alagona S, Profeta P, and Weiner P (1984) A new force field for molecular mechanical simulation of nucleic acids and proteins. *J Am Chem Soc* **106:**765–784.
Wilstermann AM and Osheroff N (2003) Stabilization of eukaryotic topoisomerase II-DNA cleavage complexes. *Curr Top Med Chem* **3:**321–338.
Zhou G (1999) *Basal Neuropharmacology*, pp 105–148, Sciences Press, Beijing.
Zhang JS, Ding J, Tang QM, Li M, Zhao M, Lu LJ, Chen LJ, and Yuan ST (1999) Synthesis and antitumour activity of novel diterpenequinone salvicine and the analogs. *Bioorg Med Chem Lett* **9:**2731–2736.

Address correspondence to: Dr. Jian Ding, Division of Antitumor Pharmacology, State Key Laboratory of Drug Research, Shanghai Institute of *Materia Medica*, Chinese Academy of Sciences, Shanghai 201203, P. R. China. E-mail: jding@mail.shcnc.ac.cn